Journal of the Serbian Chemical Society
JSCS-info@shd.org.rs • www.shd.org.rs/JSCS

ACCEPTED MANUSCRIPT

Journal of the Serbian Chemical Society
JSCS-info@shd.org.rs • www.shd.org.rs/JSCS
J. Serb. Chem. Soc. **00(0)** 1-16 (2025)
JSCS–13413
Original scientific paper
Published DD MM, 2025

A computational study to identify the metabolites in *Lippia alba* capable of inhibiting gastric cancer through BCL-2 protein inhibition

LUIS H. MENDOZA-HUIZAR*

Universidad Autónoma del Estado de Hidalgo, Academic Area of Chemistry, Carretera Pachuca-Tulancingo Km. 4.5, CP. 42184. Mineral de la Reforma, México.

(Received 7 June; revised 14 July; accepted 4 August 2025)

Abstract: In this study, a computational analysis was performed to evaluate the therapeutic potential of 73 compounds from *Lippia alba* as candidates for gastric cancer treatment. Most compounds exhibited low toxicity, except for 4-methylpent-2-enolide and β-acorenol, which demonstrated significant toxic effects. Molecular docking studies revealed that (Z)-nerolidol and 13-hydroxy-valencene both bind to the BCL2 protein, a key regulator of apoptosis in cancer cells. Furthermore, ADMET analysis predicted that both compounds are non-toxic. Molecular dynamics simulations showed that only (Z)-nerolidol maintained a stable interaction with domain 4 of BCL2, specifically with the critical Lys17 residue, which is essential for BCL2's inhibitory function. QM/MM calculations confirmed the formation of hydrogen bonds between (Z)-nerolidol and Lys17, Ile14, and Ser49, with an estimated binding energy of −62.47 kJ mol^{-1}, suggesting a stable protein-ligand complex. These findings support the potential of (Z)-nerolidol as a lead compound for BCL2 inhibition and highlight its promise as a novel therapeutic agent for gastric cancer.

Keywords: Lippia alba; molecular docking; molecular dynamics; ONIOM; PM6.

INTRODUCTION

Gastric cancer is a malignant disease that originates from the uncontrolled growth of cells lining the stomach, along with the loss of their ability to undergo apoptosis, a crucial process for eliminating abnormal cells.[1] This disease has a significant impact on public health,[2–4] and is the fourth most frequent type of cancer and the second leading cause of death worldwide.[3] The high mortality rate and increasing incidence of gastric cancer underscore the urgent need to improve existing treatments.[4–6] Current therapeutic options include radical surgery, chemotherapy, radiation therapy, targeted therapy, and immunotherapy.[4–6] Although these approaches have demonstrated effectiveness, particularly in the early stages of the disease, they are associated with significant limitations,[7,8]

* Corresponding author. E-mail: hhuizar@uaeh.edu.mx
https://doi.org/10.2298/JSC250607059M

including adverse effects,[9–11] highlighting the need to develop more selective and less toxic therapies. In this sense, an understanding of the molecular mechanisms that initiate and drive the progression of gastric cancer may help us to improve the treatments.[12]

It has been identified that the overexpression of the BCL-2 protein, associated with resistance to apoptosis and tumor development, has emerged as a key therapeutic target in gastric cancer treatment.[13] BCL-2 plays a fundamental role in regulating apoptosis, and its inhibition could promote cell death in cancerous cells. The BH3 domain of BCL-2 facilitates the formation of heterodimers with pro-apoptotic proteins like BAX, thereby inhibiting apoptosis, while the BH4 domain (residues 1 to 34) neutralizes other pro-apoptotic proteins and interacts with apoptosis regulators such as Raf-1, c-Myc, and the IP3R channel.[13] This interaction is crucial because BCL-2 inhibits the opening of the IP3R channel, reducing the release of Ca^{2+} and, consequently, apoptosis mediated by this ion.[13] Additionally, it has been suggested that the substitution of Lys17 in the BH4 domain of BCL-2 is essential for its binding and inhibition of IP3R, making Lys17 a key site for studying BCL-2 inhibition.[13] Therefore, focusing on the BH4 domain of BCL-2 presents a novel strategy, in contrast to the traditional inhibition of the BH3 domain.[13] Some studies even suggest that removing the BH4 domain from BCL-2 could turn it into a pro-apoptotic protein, similar to BAX.[13] This finding has driven the investigation of natural agents that may target the BH4 domain of BCL-2 as a potential therapeutic strategy. Accordingly, several molecular-level studies have been carried out to identify natural compounds with the potential to inhibit BCL-2.[14–18] These studies have shown that certain natural compounds can effectively act as treatments, either independently or in combination with other therapies, demonstrating promising results in the fight against gastric cancer.

In particular, metabolites from the plant *Lippia alba* have attracted attention due to their cytotoxic properties and ability to selectively induce the death of tumor cells.[19,20] *Lippia alba*, a shrub from the Verbenaceae family, is traditionally used to treat gastric and intestinal diseases and has sedative properties. The composition of *Lippia alba* essential oils varies depending on the part of the plant used, the developmental stage, and geographical conditions such as soil type and climate.[21] It has been shown that the essential oils of *Lippia alba* have a cytotoxic effect, particularly by affecting the lipid metabolism of tumor cells.[19] In addition to their action on the BCL-2 protein, these natural compounds could become effective therapeutic agents, either independently or in combination with other treatments.[1] However, although the therapeutic potential of *Lippia alba* against gastric cancer and its relationship with BCL-2 have been documented, the precise mechanism through which the plant's metabolites inhibit the protein remains unknown at the molecular level. Therefore, identifying the specific molecular interactions of these compounds with BCL-2 would allow for the prediction and evaluation of their

biological activity in the therapeutic context. In this regard, the application of ligand–receptor binding thermodynamics in drug discovery and computational chemistry constitutes a valuable tool for addressing this challenge.[22–25] Thermodynamic analysis of binding offers critical insights into the forces governing the formation of drug–target complexes.[22,23] There is now broad consensus that binding thermodynamics can serve as a key criterion throughout the various stages of ligand optimization in the development of novel therapeutic candidates.[22–25] Thus, the present study analyzes the metabolites identified in *Lippia alba* using binding thermodynamics criteria and computational tools such as ADMET studies, Lipinski's rules, molecular docking, molecular dynamics, and QM/MM methods, with the goal of identifying metabolites that may bind to the BH4 domain of the BCL-2 protein.

METHODOLOGY

In this study, we analyzed 73 metabolites from *Lippia alba,*[26,27] as potential inhibitors of the BCL-2 protein. The metabolites included are: (1) β-selinene, (2) (3Z)-hexenal, (3) (Z)-Isocitral, (4) (Z)-nerolidol, (5) 13-hydroxy-valencene, (6) 14-hydroxy-9-epi-(E)-Caryophyllene, (7) 1-methylcyclohexa-1,3-diene, (8) p-Menth-1-ene, (9) 4-methyl-2,3-dihydro-2H-pyran-6-one, (10) 5-Methylene-2-norbornene, (11) α-humulene, (12) Allo-Aromadendrene epoxide, (13) α-Pinene, (14) α-terpinene, (15) β-acorenol, (16) β-caryophyllene, (17) β-chamigrene, (18) β–elemene, (19) β-Phellandrene, (20) β-pinene, (21) Camphene, (22) Caryophyllene oxide, (23) Cis-piperitol, (24) Cis-Pinocarvyl acetate, (25) Cis-sabinene hydrate acetate, (26) Cis-ß-guaiene, (27) E-Salvene, (28) Ethyl pent-4-enoate, (29) Eugenol, (30) Eugenol acetate, (31) Exo-2-Norborneol, (32) Geranial, (33) Geraniol, (34) Geranyl acetate, (35) Geranyl butanoate, (36) Geranyl isobutanoate, (37) Geranyl formate, (38) Germacrene D, (39) Khusimol, (40) Ledol, (41) Limonene, (42) Limonene aldehyde, (43) Linalool, (44) Mesitylene, (45) Methyl eugenol, (46) Methyl geranate, (47) 1-methylcyclohexa-1,4-diene, (48) Myrcene, (49) Myrcenol, (50) Neoisodihydro carveol, (51) Neral, (52) Nerol, (53) o-Cymene, (54) p-Cymene, (55) Santalone, (56) Santolina triene, (57) Terpinolene, (58) Thuja-2,4(10)-diene, (59) Trans piperitol, (60) Trans-ascaridol glycol, (61) Trans-dihydrocarvone, (62) Trans-Piperitone epoxide, (63) Trans-verbenyl acetate, (64) Trans-β-pterpineol, (65) Tricyclene, (66) Valencene, (67) γ-Cadinene, (68) γ-Elemene, (69) γ-eudesmol, (70) γ-terpinene, (71) γ-terpineol, (72) δ-selinene, (73) δ-elemene. These metabolites were retrieved from PubChem,[28] and their IUPAC names and molecular structures are shown in Table S-1 of the supplementary material. The target protein, BCL-2, was obtained from the RCSB Protein Data Bank,[29] with the ID IG5M,[30]. Lipinski's rule of five,[31] and ADMET (Absorption, Distribution, Metabolism, Excretion, and Toxicity) parameters,[32] for all 73 metabolites were calculated using the SwissADME, [33] (Daina *et al.*, 2017) and ADMETlab[32] web servers, respectively. Molecular docking studies were conducted using the SwissDock server,[34] developed by the Swiss Institute of Bioinformatics (SIB). The compounds were evaluated based on their binding affinity (ΔG), and their interactions with protein residues were visualized using Chimera.[35] Molecular dynamics (MD) simulations were performed using GROMACS software.[36] A quantum mechanics/molecular mechanics (QM/MM) study was conducted to evaluate the electronic contributions to ligand–residue binding through the ONIOM methodology (Our own N-layered Integrated molecular Orbital and Molecular mechanics).[37] All quantum calculations presented in this work were carried out using the Gaussian 09

software,[38] and visualized with the GaussView package.[39] A list of the symbols used in this work is provided in Table S-2 of the supplementary material

RESULTS AND DISCUSSION

Analysis of metabolites according to Lipinski's rule of five and ADMET parameters

The calculation of Lipinski's Rule of Five for the 73 metabolites evaluated showed that 53 of them met the established criteria of the rule. However, the remaining 20 metabolites violated the condition of logP ≤ 4.15, suggesting possible difficulties in terms of lipophilicity and, therefore, absorption; see Table S-3 in supplementary material. Furthermore, ADMET (Absorption, Distribution, Metabolism, Excretion, and Toxicity) parameter simulations were performed for all 73 metabolites using the SwissADME[33] and ADMETlab[32] platforms. The results indicate that, in general, the 73 compounds meet at least four of the five ADMET parameters, which reinforces their potential as drug candidates. However, it is important to mention that some metabolites showed unfavorable results in particular parameters. For example, (6) 14-hydroxy-9-epi-(E)-Caryophyllene displayed an unfavorable distribution profile, which could hinder its bioavailability in the body. On the other hand, (9) 4-Methyl pent-2-enolide showed considerable toxicity, being potentially carcinogenic and corrosive to the skin and eyes. A similar profile was observed for (15) β-acorenol, which also presented adverse results related to toxicity, which is a critical factor to consider during the selection process of metabolites for drug development.

Active site prediction on 1G5M

Drug efficacy often depends on binding to specific protein sites, traditionally identified from static structures. However, this approach overlooks protein dynamics. Cryptic pockets, transient or hidden cavities revealed through conformational changes, can be uncovered using molecular dynamics simulations, offering new targets for drug development.[40] Cryptic pockets can be identified using advanced methods such as molecular simulations, artificial intelligence, or high-resolution experimental techniques.[40] In this study, we conducted a comparative analysis to identify binding sites in the static structure of the BCL-2 protein (PDB ID: 1G5M) and contrasted them with cryptic pockets predicted using deep neural networks. The active sites of the static BCL-2 structure were predicted using the PrankWeb server (https://prankweb.cz/),[41] which identified six potential binding sites (Figure 1a). Each of these predicted pockets exhibited varying probabilities of ligand binding, with pocket 1 showing the highest probability (0.326), followed by pockets 2 (0.134), 3 (0.087), 4 (0.039), 5 (0.033), and 6 (0.033). In terms of binding affinity, pocket 1 demonstrated the highest score (6.10), followed by pockets 2 (3.52), 3 (2.79), 4 (1.94), 5 (1.81), and 6 (1.80). These scores indicate predicted binding strength, with higher values suggesting stronger ligand interactions. This pattern supports the hypothesis that pocket 1 is

the most biologically relevant binding site. Here, it is important to note that the BH4 domain (residues 1–34) has some overlap with pocket 1. However, residue Lys17, located in this domain and experimentally shown to be essential for IP3R inhibition,[13] is not included in any of the pockets identified in the static structure. The cryptic pockets of BCL-2 were predicted using the PocketMiner server (https://pocketminer.azurewebsites.net/), which employs deep neural networks to predict where transient pockets may form during molecular dynamics simulations.[40] The results are shown in Figure 1b, where residues highlighted in red and blue correspond to regions with high probabilities of cryptic pocket formation. Importantly, these regions are located within the BH4 domain, indicating a potential functional role for this domain in ligand binding. Two main subregions were identified: pocket 1a and pocket 1b. Notably, pocket 1b overlaps with static pocket 1, while pocket 1a includes Lys17 which is an experimentally validated key residue involved in IP3R inhibition.

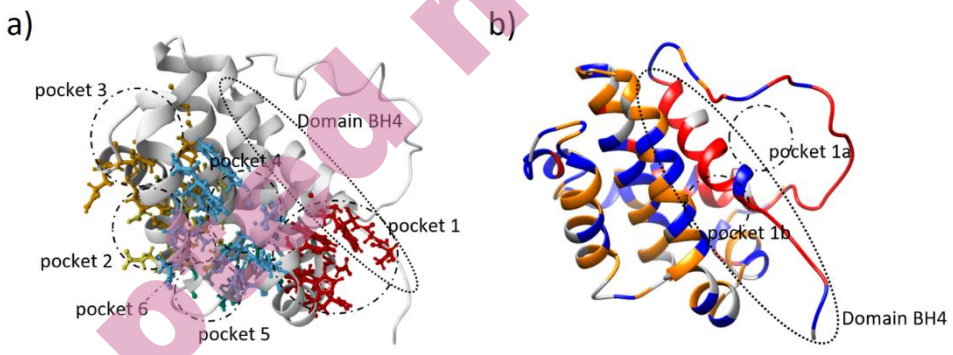

Figure 1. Active sites on 1G5M a) static structure b) cryptic sites.

Binding analysis of Lippa alba metabolites with 1G5M through a molecular docking study.

Molecular docking studies were performed using the SwissDock server[34], developed by the Swiss Institute of Bioinformatics (SIB). This server automatically assigns docking parameters, such as box size and affinity evaluation methods, employing a rigid-flexible docking approach. Prior to docking, the protein structure was prepared by removing all solvent molecules and receptor-binding chemicals to focus the docking process on the protein's essential interaction sites. The compounds were assessed based on their binding affinity (ΔG), and their interactions with protein residues were visualized using Chimera.[35] These visualizations provide valuable insights into how metabolites interact with the target protein, aiding in the identification of potential inhibitors. To further

explore the role of metabolite structure in inhibiting BCL-2 for the treatment of gastric cancer, the optimal ligand/protein configuration and binding affinities of each metabolite were evaluated. This analysis is essential for understanding how structural variations in metabolites influence their ability to effectively interact with BCL-2, which is critical for therapeutic development. Furthermore, evaluating the binding affinity helps to identify metabolites with higher therapeutic potential for BCL-2 inhibition, thereby contributing to the development of more effective treatments for gastric cancer. The binding free energy (ΔG) values for the 73 compounds analyzed are presented in Figure 2. Metabolite (9), 4-methylpent-2-enolide, exhibits the strongest binding affinity with a ΔG of -31.13 kJ mol^{-1}, followed by compound (5), 13-hydroxy-valencene (ΔG = -30.29 kJ mol^{-1}), and compound (4), (Z)-nerolidol (ΔG = -30.25 kJ mol^{-1}). It is noteworthy that 4-methylpent-2-enolide specifically binds to the BH4 domain of BCL-2, interacting with residue LYS17 within pocket 1a, as shown in Figure 1a. In contrast, compound (4) binds within pocket 1, while compound (5) is also located in the BH4 domain, near pocket 1a. From a pharmacological perspective, compound (4) has been widely reported for its anti-inflammatory, antioxidant, and antimicrobial properties,[26,27] making it a promising candidate for future therapeutic applications. Similarly, compound (5) exhibits antioxidant and anti-inflammatory activities and interacts directly with residue Lys17. In contrast, no known therapeutic properties have been reported for compound (9). Furthermore, ADMET analysis indicates that this metabolite has significant toxicity, being potentially carcinogenic and corrosive to skin and mucous membranes, which severely limits its therapeutic potential. At the molecular level, both compounds (5) and (9) display similar interactions with Lys17, including hydrogen bonds, π-alkyl, and π-sigma interactions, reinforcing the importance of this residue as an active site within the BH4 domain. However, compound (4), despite binding outside pocket 1a and within pocket 1, does so in a region that represents the most accessible binding site in the static structure, although it initially does not establish direct interactions with Lys17. Collectively, these findings suggest that compounds (4) and (5) possess greater therapeutic potential compared to compound (9), as they not only exhibit favorable binding affinity but also interact with key regions of BCL-2 associated with functional inhibition. Moreover, compounds (4) and (5) exhibit binding energies comparable to that of baicalin with BCL2 (−38.5 kJ mol^{-1}), as reported in previous *in silico* studies, highlighting their potential as anticancer agents. This supports their potential development as effective BCL-2 inhibitors for future research.[42] The dissociation (K_d) and binding (K_B) constants were evaluated for compounds (4) ((Z)-nerolidol) and (5) (13-hydroxy-valencene), respectively. The dissociation constant is related to the standard Gibbs free energy change according to the following equation:[43,44]

$$K_{\mathrm{d}} = \mathrm{e}^{\frac{\Delta_{\mathrm{B}}G^{0}}{\mathrm{RT}}} \quad (1)$$

In contrast, the binding constant (K_B) is the inverse of the dissociation constant and is calculated as:[43,44]

$$K_{\mathrm{B}} = \mathrm{e}^{-\frac{\Delta_{\mathrm{B}}G^{0}}{\mathrm{RT}}} \quad (2)$$

Based on the binding free energy values, which were −30.23 kJ·mol^{-1} for (Z)-nerolidol and −30.30 kJ·mol^{-1} for 13-hydroxy-valencene, the K_d and K_B values were determined. For (Z)-nerolidol, K_d was 5.11 × 10^{-6} M and K_B was 1.96 × 10^{5} M^{-1}; whereas for 13-hydroxy-valencene, the values were 4.96 × 10^{-6} M and 2.02 × 10^{5} M^{-1}, respectively. The negative ΔG_B values for both compounds indicate that the binding is spontaneous and thermodynamically favorable. Moreover, the dissociation constants (K_d) in the low micromolar range suggest a moderately high affinity between (Z)-nerolidol and 13-hydroxy-valencene and BCL2. The slight difference observed between the two compounds suggests that 13-hydroxy-valencene has a slightly higher affinity (lower K_d and higher K_B), which may be attributed to minor structural variations that enhance its interaction with the active site. These values of K_d and K_B evaluated in this work fall within the range reported for BCL2 inhibition.[30,45]

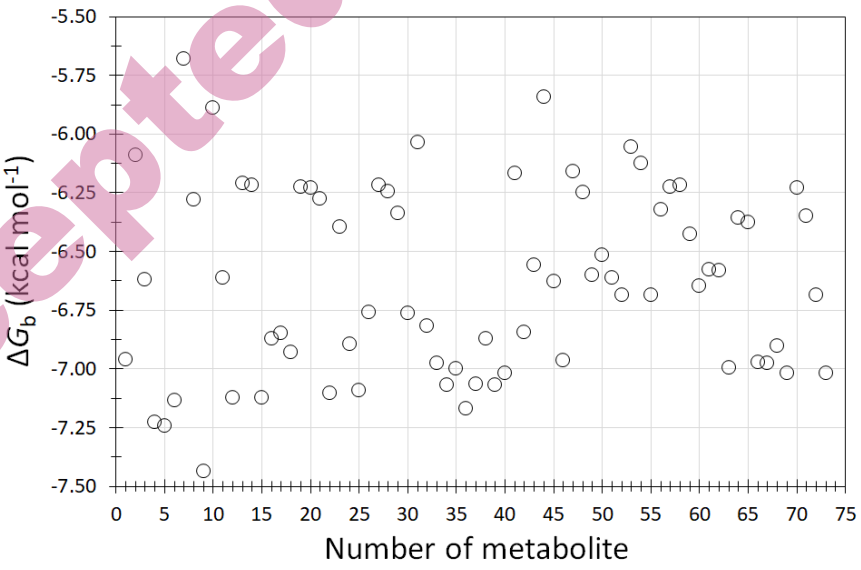

Figure 2. $\Delta_B G$ of binding between *Lippia alba* metabolites and 1G5M.

Analysis of the stability of compounds 13-hydroxy-valencene, and (Z)-nerolidol in complex with 1G5M through a molecular dynamics study.

To analyze the stability of compounds (Z)-nerolidol and 13-hydroxy-valencene binding to the BH4 domain of BCL-2 and its interaction with Lys17, molecular dynamics (MD) simulations were performed using the GROMACS software.[36] These simulations were set up by constructing a simulation box with a 1 Å margin, ensuring charge neutrality, and adding water molecules (TIP3P model) to fill the system, which was centered within a cubic box. Initially, energy minimization was performed to achieve the most stable conformation, ensuring a reasonable starting structure in terms of geometry and solvent orientation. The system was then subjected to two stages. The first one stage was performed under an NVT ensemble, allowing the system's temperature to stabilize at 300 K. The second stage involved pressure equilibration under an NPT ensemble for 1 ns. The stability of the BCL-2 complexes with (Z)-nerolidol and 13-hydroxy-valencene was evaluated throughout the 100 ns simulation. Figure 3 shows the RMSD vs. simulation time graphs for these compounds. In the case of BCL2-13-hydroxy-valencene, it was displaced from pocket 1a; initially, some interactions with Lys17 at the first nanoseconds were observed; however, at the simulation proceeded, these interactions were lost, and the compound migrated to another site different from those schematized in Figure 1. For complex BCL2-(Z)-nerolidol, the system exhibited an important fluctuation of approximately 0.8 nm at 7 ns, after which it remained stable until 100 ns. At 7 ns, compound (Z)-nerolidol migrates and binds from pocket 1 to pocket 1a and remains stable to 100 ns. The interactions of this complex are detailed in Table 1, where it can be observed that there is stable binding with the active site Lys17 during 100 ns. These results suggest that (Z)-nerolidol has more therapeutic possibilities than 13-hydroxy-valencene.

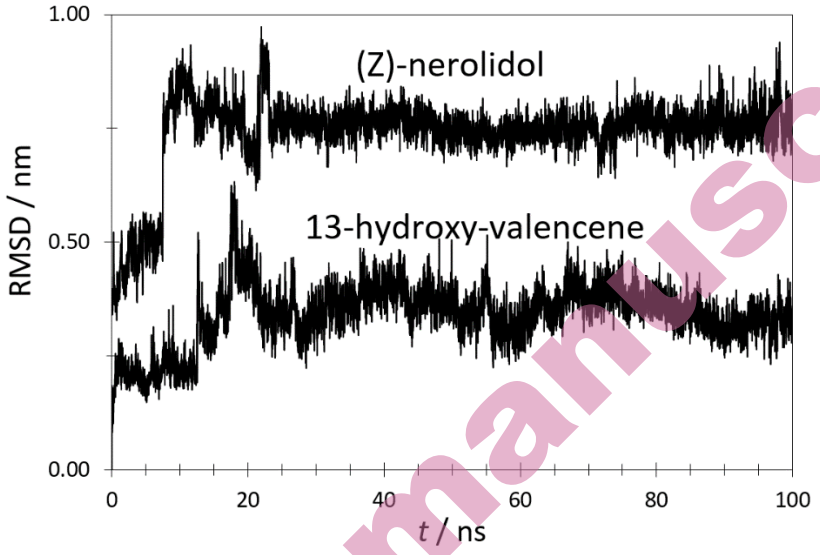

Figure 3. RMSD plots from molecular dynamics simulations of the 1G5M-ligand complexes involving compounds (Z)-nerolidol and 13-hydroxy-valencene.

Table 1. Residues interacting with compound (Z)-nerolidol during the molecular dynamics simulation at selected time points. Only residues within interaction distance (<4.0 Å) were included.

t / ns	Residues
0	His20, Tyr21, His94, Val93, Ile14, Tyr9, Lys17, Tyr18
10	His20, Val93, Ile14, Tyr9, Lys17
20	His20, Val93, Ile14, Tyr9, Lys17
30	His94, Val93, Tyr9, Lys17
40	His20, His94, Val93, Ile14, Tyr9, Lys17
50	His94, Val93, Ile14, Tyr9, Lys17, Tyr18
60	His94, Val93, Ile14, Tyr9, Lys17
70	Tyr21, His94, Val93, Ile14, Tyr9, Lys17
80	Tyr 21, His94, Ile14, Tyr9, Lys17, Tyr18
90	His20, His94, Val93, Ile14, Tyr9, Lys17, Tyr18
100	His20,Tyr21,His94,Val93,Ile14,Tyr9,Lys17

Also, it was observed stable and persistent interaction between (Z)-nerolidol and residues Lys17, Ile14, Tyr9, Val93, and His94 throughout the molecular dynamics simulations. Interactions with Lys17 and Ile14 engage in hydrogen bonding, while Tyr9 contributes through π-alkyl interactions. Both types of interactions appear to play a critical role in maintaining the integrity of the ligand-protein complex.

Analysis of the molecular interactions between (Z)-nerolidol and 1G5M through ONIOM quantum calculations.

The molecular dynamics study revealed that compound (Z)-nerolidol remains stable within pocket 1a of the BCL2 protein, forming predominant interactions with residues Lys17, Ile14, Tyr9, Val93, and His94. To further characterize these interactions and understand their electronic basis, a hybrid QM/MM study was performed. Due to the size of the protein–ligand system, which makes a full quantum mechanical treatment computationally impractical, the ONIOM methodology was employed.[37] This approach enables accurate modeling of the active site region while maintaining a reasonable computational cost. In the applied ONIOM model, both the ligand and the residues directly involved in the active site interactions (Lys17, Ile14, Tyr9, Val93, and Ser49) were included in the high-level quantum mechanical (QM) region, while the rest of the system was treated using molecular mechanics (MM) (Figure 4). Here, it is important to mention that the selection of the theoretical levels for the QM and MM regions is fundamental for accurately calculating the properties of interest. In this context, density functional theory (DFT) calculations, while generally more accurate than semiempirical methods, can become computationally prohibitive when attempting to analyze noncovalent interactions in detail, particularly in large or flexible molecular systems such as protein-ligand complexes. In this sense, the literature reports that, for biomolecular systems or noncovalent complexes, semiempirical methods can provide reasonably accurate results at a fraction of the computational cost of DFT.[46] However, the deviations from experimental data are greater when using semiempirical methods than with DFT.[47] Considering the advantages of PM6 in reproducing experimental trends at a lower computational cost compared to DFT, in the present work the system geometry was optimized using the semiempirical PM6 method for the quantum mechanical region,[48] and the Universal Force Field (UFF) for the molecular mechanics region.[49] This combination of these theoretical levels has proven suitable and accuracy for describing the structural and electronic features of novel metal–Schiff base complexes derived from allylamine, as well as their interactions with human serum albumin, in the context of anticancer drug discovery.[50] As a result of the geometry optimization, a network of non-classical hydrogen bonds and π–alkyl interactions was identified between (Z)-nerolidol and several key residues within the binding site of 1G5M. Detailed analysis revealed an intramolecular hydrogen bond of 2.3 Å between the carbonyl oxygen atom of Lys17 and a hydrogen atom belonging to a methyl group of the (Z)-nerolidol moiety, indicative of a C–O···H–C interaction. Although such interactions are generally weaker than classical hydrogen bonds, they can significantly contribute to ligand conformational stability and binding specificity.[51] A second C–O···H–C interaction was observed between the carbonyl oxygen of Lys17 and a hydrogen atom attached to carbon 4 of (Z)-nerolidol. Additionally, the carbonyl oxygen of

Ile14 forms a weaker hydrogen bond (O···H, 2.4 Å) with a hydrogen atom from the methyl group at position 7 of (Z)-nerolidol. This interaction, also classified as a C–H···O non-classical hydrogen bond, is predominantly electrostatic in nature,[51] but still plays a relevant role in orienting the ligand within the binding pocket. A longer and weaker intramolecular hydrogen bond was observed between the carbonyl oxygen of Ser49 and the hydrogen atom at carbon 9 of the ligand, with a distance of 3.2 Å. This interaction is also mainly electrostatic, and while it contributes modestly to the overall binding affinity, it still supports the spatial orientation of the ligand.[51] These interactions were visualized using Discovery Studio Visualizer,[52] and are depicted in Figure S-1 in the supplementary material. Also, a π–alkyl interaction was identified between the π-electron cloud of the aromatic ring of Tyr9 and the terminal methyl group of (Z)-nerolidol, with a contact distance of 3.1 Å. Additional alkyl interactions were found between the methyl group of (Z)-nerolidol and Val93, with distances of 2.4 and 2.6 Å, respectively. A further alkyl interaction was observed between the methyl group of (Z)-nerolidol and His94, at a distance of 2.1 Å, involving hydrogen atoms from the ligand's methyl group and the imidazole ring of the residue. The binding energy (E_B)was evaluated from these ONIOM calculations through the following equation:

$$E_B = E_{complex} - \left(E_{protein} + E_{ligand}\right) \quad (3)$$

The $E_{complex}$ is -5.531177 hartrees, $E_{protein}$=-5.41322 hartrees and E_{ligand} = 0.094161 hartrees. Thus, the E_B=-0.023796 hartrees or -62.48 kJ mol^{-1}. This value indicates a favorable interaction and suggests the formation of a stable complex between BCL2 and compound (4), supporting its potential as an inhibitor.

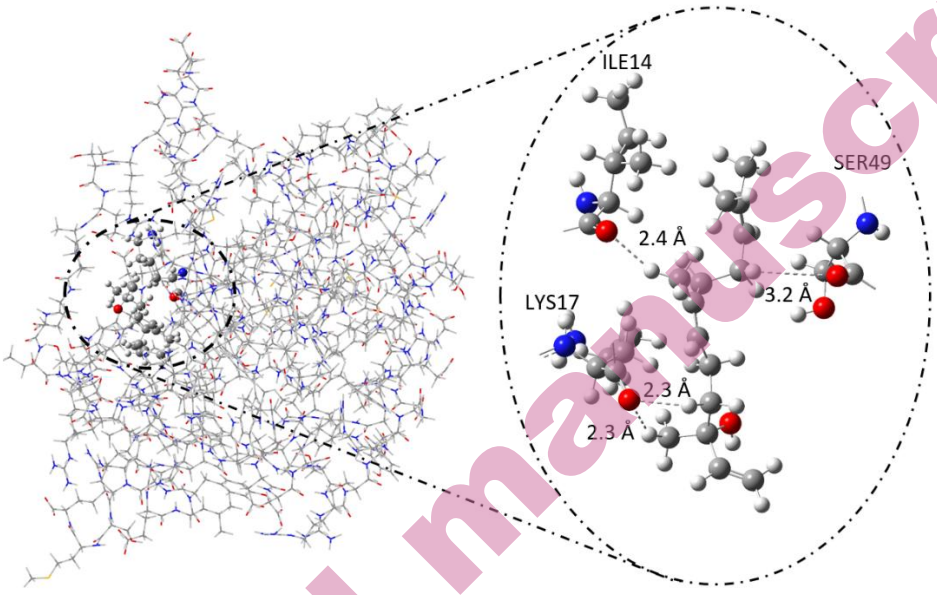

Figure 4. ONIOM model applied to the BCL2-(Z)-nerolidol complex. The high-level (QM) region includes the ligand and key residues Lys17, Ile14, and Ser49. Hydrogen bond distances are shown in Å.

CONCLUSION

In this study, 73 metabolites present in the plant *Lippia alba* were evaluated, which were analyzed using Lipinski's rules and ADMET properties to assess their potential as drugs and their toxicity. Of these 73 compounds, molecular docking revealed that the compounds (Z)-nerolidol and 13-hydroxy-valencene interact with the Lys17 residue, identified as essential for binding and inhibition of IP3R in the BH4 domain of BCL-2. The molecular dynamics study indicated that only the compound (Z)-nerolidol maintains a stable binding with Lys17 for 100 ns. In particular, (Z)-nerolidol showed stable and specific interactions with key residues, which was confirmed through ONIOM calculations. These results support its potential as a lead candidate for the development of BCL2 inhibitors and justify its experimental evaluation in future studies.

SUPPLEMENTARY MATERIAL

Additional data are available electronically at the pages of journal website: https://www.shd-pub.org.rs/index.php/JSCS/article/view/13413, or from the corresponding author on request.

Acknowledgements: LHMH thankfully acknowledges the computer resources, technical expertise, and support provided by the Laboratorio Nacional de Supercómputo del Sureste de México, CONACYT member of the network of national laboratories through the project No.

202501011N. Guanajuato National Laboratory (CONACyT 123732) is acknowledged for supercomputing resources. LHMH thanks the Universidad Autónoma del Estado de Hidalgo for the support granted for this work. LHMH acknowledges to the SNII for the distinction of his membership and the stipend received.

ИЗВОД

РАЧУНАРСКА СТУДИЈА ЗА ИДЕНТИФИКАЦИЈУ МЕТАБОЛИТА У *LIPPIA ALBA* СПОСОБНИХ ДА ИНХИБИРАЈУ РАК ЖЕЛУЦА ПУТЕМ ИНХИБИЦИЈЕ *BCL-2* ПРОТЕИНА

LUIS H. MENDOZA-HUIZAR

Universidad Autónoma del Estado de Hidalgo, Academic Area of Chemistry, Carretera Pachuca-Tulancingo Km. 4.5, CP. 42184. Mineral de la Reforma, México.

У овој студији спроведена је рачунарска анализа како би се проценио терапеутски потенцијал 73 једињења из биљке *Lippia alba* као потенцијалних кандидата за лечење рака желуца. Већина једињења има ниску токсичност, изузев 4-метилпент-2-енолида и β-акоренола, који имају значајне токсичне ефекте. Докинг анализа показала је да се (*Z*)-неролидол и 13-хидрокси-валенцен везују за BCL-2 протеин, кључни регулатор апоптозе у ћелијама карцинома. Додатно, ADMET анализа је предвидела да су оба једињења нетоксична. Молекулска динамика је показала да само (Z)-неролидол одржава стабилну интеракцију са доменом 4 протеина BCL-2, посебно са критичним Lys17 остатком, који је од суштинске важности за инхибиторну функцију BCL-2. QM/MM прорачуни су потврдили формирање водоничних веза између (Z)-неролидола и аминокиселинских остатака Lys17, Ile14 и Ser49, са процењеном енергијом везивања од −62.47 kJ mol^{-1}, што указује на стабилан протеин-лиганд комплекс. Ови резултати указују на потенцијал (*Z*)-неролидола као водећег једињења за инхибицију BCL-2 и истичу његов значај као новог терапеутског агенса за лечење рака желуца.

(Примљено 7. јуна; ревидирано 30. марта; прихваћено 4. августа 2025.)

REFERENCES

1. A. Sarkar, A. Paul, T. Banerjee, A. Maji, S. Saha, A. Bishayee, T. K. Maity, *Eur. J. Pharmacol.* **944** (2023) 175588 (http://dx.doi.org/10.1016/J.EJPHAR.2023.175588)
2. H. R. Khouzani, M. R. Maleki, A. Zackery, E. Mazloumi, M. Jalilzadeh, M. Sahebzadeh, *Heliyon* **10** (2024) e40437 (http://dx.doi.org/10.1016/J.HELIYON.2024.E40437)
3. M. Ilic, I. Ilic, *World J. Gastroenterol.* **28** (2022) 1187–1203 (http://dx.doi.org/10.3748/WJG.V28.I12.1187)
4. R. Panahizadeh, P. Panahi, V. Asghariazar, S. Makaremi, G. Noorkhajavi, E. Safarzadeh, *Cancer Cell Int. 2025 251* **25** (2025) 1–20 (http://dx.doi.org/10.1186/S12935-025-03655-8)
5. E. Morgan, M. Arnold, M. C. Camargo, A. Gini, A. T. Kunzmann, T. Matsuda, F. Meheus, R. H. A. Verhoeven, J. Vignat, M. Laversanne, J. Ferlay, I. Soerjomataram, *EClinicalMedicine* **47** (2022) 101404 (http://dx.doi.org/10.1016/J.ECLINM.2022.101404)
6. T. I. Mamun, S. Younus, M. H. Rahman, *Cancer Treat. Res. Commun.* **41** (2024) 100845 (http://dx.doi.org/10.1016/J.CTARC.2024.100845)

7. S. S. Joshi, B. D. Badgwell, *CA. Cancer J. Clin.* **71** (2021) 264 (http://dx.doi.org/10.3322/CAAC.21657)
8. Q. Yin, Y. Zhang, X. Xie, M. Hou, X. Chen, J. Ding, *Cell Death Discov. 2025 111* **11** (2025) 1–17 (http://dx.doi.org/10.1038/s41420-025-02429-5)
9. B. Zhao, W. Lv, J. Lin, *Curr. Probl. Cancer* **44** (2020) 100577 (http://dx.doi.org/10.1016/J.CURRPROBLCANCER.2020.100577)
10. W. Leowattana, P. Leowattana, T. Leowattana, F. Professor, *World J. Methodol.* **13** (2023) 79 (http://dx.doi.org/10.5662/WJM.V13.I3.79)
11. D. Luo, Y. Liu, Z. Lu, L. Huang, *Mol. Med. 2025 311* **31** (2025) 1–27 (http://dx.doi.org/10.1186/S10020-025-01075-Y)
12. C. D. Iwu, C. J. Iwu-Jaja, *Hyg. 2023, Vol. 3, Pages 256-268* **3** (2023) 256–268 (http://dx.doi.org/10.3390/HYGIENE3030019)
13. Z. Liu, C. Wild, Y. Ding, N. Ye, H. Chen, E. A. Wold, J. Zhou, *Drug Discov. Today* **21** (2016) 989–996 (http://dx.doi.org/10.1016/j.drudis.2015.11.008)
14. Y. Qu, X. Yang, J. Li, S. Zhang, S. Li, M. Wang, L. Zhou, Z. Wang, Z. Lin, Y. Yin, J. Liu, N. Wang, Y. Yang, *Evid. Based. Complement. Alternat. Med.* **2021** (2021) 2311486 (http://dx.doi.org/10.1155/2021/2311486)
15. Y. Q. Ma, M. Zhang, Z. H. Sun, H. Y. Tang, Y. Wang, J. X. Liu, Z. X. Zhang, C. Wang, *World J. Gastrointest. Oncol.* **16** (2024) 493 (http://dx.doi.org/10.4251/WJGO.V16.I2.493)
16. N. Bahadar, S. Bahadar, A. Sajid, M. Wahid, G. Ali, A. Alghamdi, H. Zada, T. Khan, S. Ullah, Q. Sun, *Breast Cancer Res.* **26** (2024) 114 (http://dx.doi.org/10.1186/S13058-024-01868-9)
17. K. Kai, J. Han-bing, C. Bing-lin, Z. Shu-jun, *Heliyon* **9** (2023) e17393 (http://dx.doi.org/10.1016/J.HELIYON.2023.E17393)
18. S. Dey, A. K. Singh, S. Kumar, *Biointerface Res. Appl. Chem.* **13** (2022) 1–12 (http://dx.doi.org/10.33263/BRIAC135.473)
19. S. Montero Villegas, J. F. Ciccio Alberti, X. Cortés Bratti, R. Crespo, M. Polo, M. García de Bravo, *Terc. Epoca. Rev. Cient. La Fcaultad Ciencias Médicas* **2** (2010) 1–1. (http://sedici.unlp.edu.ar/handle/10915/15469)
20. M. Á. Ramírez-García, J. E. Márquez-González, Horacio Barranco-Lampón, Gilberto López-Aguilar, *El Resid.* **9** (2014) 84–94 (http://dx.doi.org/10.5754/hge11946)
21. E. E. Stashenko, B. E. Jaramillo, J. R. Martínez, *Rev. Acad. Colomb. Ciencias* **27** (2003) 579–597 (http://dx.doi.org/10.18257/ssn.0370-3908)
22. R. Claveria-Gimeno, S. Vega, O. Abian, A. Velazquez-Campoy, *Expert Opin. Drug Discov.* **12** (2017) 363–377 (http://dx.doi.org/10.1080/17460441.2017.1297418)
23. X. Du, Y. Li, Y. L. Xia, S. M. Ai, J. Liang, P. Sang, X. L. Ji, S. Q. Liu, *Int. J. Mol. Sci.* **17** (2016) 1–34 (http://dx.doi.org/10.3390/ijms17020144)
24. M. E. Popović, V. Tadić, M. Popović, *Virology* **603** (2025) (http://dx.doi.org/10.1016/j.virol.2024.110319)
25. W. López-Orozco, L. H. Mendoza-Huizar, G. A. Álvarez-Romero, J. de Jesús Martin Torres-Valencia, *J. Serbian Chem. Soc.* **90** (2025) 291–303 (http://dx.doi.org/10.2298/JSC240428074L)
26. L. Silva-Santos, L. Palhares Neto, N. Corte-Real, M. V. L. Sperandio, C. A. G. Camara, M. M. Moraes, C. Ulisses, *South African J. Bot.* **163** (2023) 756–769 (http://dx.doi.org/10.1016/j.sajb.2023.10.024)

27. P. T. de Souza Silva, L. M. de Souza, M. B. de Morais, M. M. de Moraes, C. A. G. da Camara, C. Ulisses, *South African J. Bot.* **147** (2022) 415–424 (http://dx.doi.org/10.1016/j.sajb.2022.01.042)
28. S. Kim, J. Chen, T. Cheng, A. Gindulyte, J. He, S. He, Q. Li, B. A. Shoemaker, P. A. Thiessen, B. Yu, L. Zaslavsky, J. Zhang, E. E. Bolton, *Nucleic Acids Res.* **53** (2025) D1516–D1525 (http://dx.doi.org/10.1093/NAR/GKAE1059)
29. H. M. Berman, J. Westbrook, Z. Feng, G. Gilliland, T. N. Bhat, H. Weissig, I. N. Shindyalov, P. E. Bourne, *Nucleic Acids Res.* **28** (2000) 235–242 (http://dx.doi.org/10.1093/NAR/28.1.235)
30. A. M. Petros, A. Medek, D. G. Nettesheim, D. H. Kim, H. S. Yoon, K. Swift, E. D. Matayoshi, T. Oltersdorf, S. W. Fesik, *Proc. Natl. Acad. Sci. U. S. A.* **98** (2001) 3012–3017 (http://dx.doi.org/10.1073/pnas.041619798))
31. C. A. Lipinski, *Drug Discov. Today Technol.* **1** (2004) 337–341 (http://dx.doi.org/10.1016/J.DDTEC.2004.11.007)
32. G. Xiong, Z. Wu, J. Yi, L. Fu, Z. Yang, C. Hsieh, M. Yin, X. Zeng, C. Wu, A. Lu, X. Chen, T. Hou, D. Cao, *Nucleic Acids Res.* **49** (2021) W5–W14 (http://dx.doi.org/10.1093/nar/gkab255)
33. A. Daina, O. Michielin, V. Zoete, *Sci. Rep.* **7** (2017) 1–13 (http://dx.doi.org/10.1038/srep42717)
34. A. Grosdidier, V. Zoete, O. Michielin, *Nucleic Acids Res.* **39** (2011) W270 (http://dx.doi.org/10.1093/NAR/GKR366)
35. E. F. Pettersen, T. D. Goddard, C. C. Huang, G. S. Couch, D. M. Greenblatt, E. C. Meng, T. E. Ferrin, *J. Comput. Chem.* (2004) (http://dx.doi.org/10.1002/jcc.20084)
36. M. J. Abraham, T. Murtola, R. Schulz, S. Páll, J. C. Smith, B. Hess, E. Lindah, *SoftwareX* **1–2** (2015) 19–25 (http://dx.doi.org/10.1016/J.SOFTX.2015.06.001)
37. M. Svensson, S. Humbel, R. D. J. Froese, T. Matsubara, S. Sieber, K. Morokuma, *J. Phys. Chem.* **100** (1996) 19357–19363 (http://dx.doi.org/10.1021/JP962071J;CTYPE:STRING:JOURNAL)
38. Gaussian 09, Revision A.01, Gaussian, Inc., Wallingford, CT, 2009. (https://gaussian.com/g09citation/)
39. Gaussview Rev. 3.09, Windows version. Gaussian Inc., Pittsburgh, PA. (https://gaussian.com/508_gvw/)
40. A. Meller, M. Ward, J. Borowsky, M. Kshirsagar, J. M. Lotthammer, F. Oviedo, J. L. Ferres, G. R. Bowman, *Nat. Commun.* **14** (2023) (http://dx.doi.org/10.1038/s41467-023-36699-3)
41. L. Jendele, R. Krivak, P. Skoda, M. Novotny, D. Hoksza, *Nucleic Acids Res.* **47** (2019) W345–W349 (http://dx.doi.org/10.1093/nar/gkz424)
42. V. Sharma, A. Gupta, M. Singh, A. Singh, A. A. Chaudhary, Z. H. Ahmed, S. U. D. Khan, S. Rustagi, S. Kumar, S. Kumar, *Front. Bioinforma.* **5** (2025) 1–13 (http://dx.doi.org/10.3389/fbinf.2025.1545353)
43. M. Popovic, *Virology* **570** (2022) 35–44 (http://dx.doi.org/10.1016/j.virol.2022.03.008)
44. M. Popovic, *Microb. Risk Anal.* **22** (2022) 100231 (http://dx.doi.org/10.1016/j.mran.2022.100231)
45. E. Wolf, C. Lento, J. Pu, B. C. Dickinson, D. J. Wilson, *Biochemistry* **62** (2023) 1619–1630 (http://dx.doi.org/10.1021/acs.biochem.2c00709)
46. J. Fanfrlík, A. K. Bronowska, J. Řezáč, O. Přenosil, J. Konvalinka, P. Hobza, *J. Phys. Chem. B* **114** (2010) 12666–12678 (http://dx.doi.org/10.1021/JP1032965)

47. J. Řezáč, J. Fanfrlík, D. Salahub, P. Hobza, *J. Chem. Theory Comput.* **5** (2009) 1749–1760 (https://doi.org/10.1021/ct9000922)
48. J. J. P. Stewart, *J. Mol. Model.* **13** (2007) 1173–1213 (http://dx.doi.org/10.1007/s00894-007-0233-4)
49. A. K. Rappé, C. J. Casewit, K. S. Colwell, W. A. Goddard, W. M. Skiff, *J. Am. Chem. Soc.* **114** (1992) 10024–10035 (https://doi.org/10.1021/ja00051a040)
50. Z. Kazemi, H. A. Rudbari, M. Sahihi, V. Mirkhani, M. Moghadam, S. Tangestaninejad, I. Mohammadpoor-Baltork, S. Gharaghani, *J. Photochem. Photobiol. B Biol.* **162** (2016) 448–462 (http://dx.doi.org/10.1016/J.JPHOTOBIOL.2016.07.003)
51. G. R. . Desiraju, T. Steiner, *The weak hydrogen bond : in structural chemistry and biology*, Oxford University Press, 2001
52. Biovia Dassault Systèmes, *Discovery Studio Visualiser 2019*, Dassault Systèmes, San Diego, 2020 (http://dx.doi.org/https://discover.3ds.com/discovery-studio-visualizer-download).